 SDHM, vol.9, no.1, pp.43-66, 2013

Intra-laminar Damage Evolution in a Composite Grid Structure Representative Volume Element under Compression Load

A. Riccio[1], **F. Caputo**[1] **and N. Tessitore**[2]

Abstract: In this paper the mechanical behavior of composites grid structures has been numerically investigated. The evolution of fibers and matrix cracking has been simulated by adopting a progressive damage approach. The Hashin failure criteria and ply properties degradation rules have been adopted to simulate the degradation at ply level. Non-linear analyses on a Representative Volume Element of the composite grid structure have been performed to account for its compression behavior.

Keywords: Progressive damage, grid structures, FEM, buckling, RVE.

1 Introduction

Due to the relevant difficulties in the manufacturing process, for many years the composite grid structures have not been considered as a valid alternative to standard aerospace structural concepts. However, in the last years, remarkable progresses have been made in the manufacturing of composite grids so that they are being strongly reconsidered for aerospace applications (Vasiliev, Barynin, and Rasin 2001; Vasiliev, and Razin 2006; Hou, and Gramoll 2000). Grid structures are characterized by a shell structure (or skin) supported by a lattice pattern (or grid) of rigid and interconnected ribs (Buragohain, and Velmurugan 2011). Fibrous composite materials seem to be particularly suitable for grid structure applications due to their high directionality which allows the material's stiffness and strength to be driven along the rib directions according to stresses gradients. The chance to easily automate the manufacturing process is another advantage of composite grid structures. As an example, the automated filament winding manufacturing process is widely adopted for the manufacturing of revolution grid structures used for aerospace applications (Huybrechts, Meink, Wegner, and Ganley 2002). Nevertheless, one ma-

[1] The Second University of Naples - DIAM, Naples, Italy.
[2] AVIO, Colleferro (Rome), Italy.

jor drawback, which can negatively influence the introduction of the composite grid structure into industry, is the lack of understanding about the onset and propagation of damage within the grids components (ribs and skin) under compressive loading conditions which may be very critical for the integrity of the single components and for the interface skin-ribs. The compressive behavior of composites grid structures has been investigated by Kidane, Helms, Pang, and Woldesenbet (2003) and by Wodesenbet, Kidane, and Pang (2003) where an analytical model for determination of the stiffness of a grid stiffened composite cylindrical shell has been developed by taking into account a grid representative volume element (RVE). Well established stress based failure criteria can be found in literature which account for the damage on-set in terms of fiber and matrix cracking in composite materials. The Hashin-Rotem criterion (Hashin 1980; Hashin, and Rotem 1973), being able to distinguish between fiber breakage and matrix cracking, seems to be the most reliable one in interpreting the material physical behavior. Other failure criteria (Yamada, and Sun 1978; Christensen 1988; Tsai, and Wu 1971; Feng 1991), even if effective in FE implementation, lack in terms of composite failure mechanism description.

In order to simulate the damage evolution, a progressive failure procedure involving failure criteria and material properties degradation rules is needed. The basic description of a progressive failure procedure is presented by Ochoa, and Reddy (1992); Sleight, Knight, and Wang (1997) and Sleight (1999) where the application of the failure criteria and the description of the material properties after the damage detection are appointed as key aspects. In general three categories of material degradation models can be identified: instantaneous unloading (Murray, and Schwer 1990), gradual unloading (Petit, and Waddoups 1969; Sandhu 1974; Nahas 1986) and constant stress at ply failure (Hahn, and Tsai 1983). Progressive failure analyses on composites grid structures have been performed by He, and He (2010) and by Zhang, Chen, and Ye (2008) where the combinations Tsai-Wu failure criterion /Chang stiffness degradation criterion and Hashin criterion /instantaneous degradation rules have been respectively used, however, no information is given about the damage evolution under compressive loading conditions. Additional examples of progressive failure analysis are reported in Katerelos, Kashtalyan, Soutis, and Galiotis (2008), where the effect of matrix cracking on the behavior of glass/epoxy laminates loaded statically in tension has been investigated, and in Soutis, and Kashtalyan (2011) where the Equivalent Constraint Model (ECM) is applied to predict residual stiffness properties of polymer matrix cross-ply laminates subjected to in-plane biaxial loading and damaged by matrix cracks. An interesting review of some progression damage models is presented in Kashtalyan, and Soutis (2005) where the failure process of composite laminate involving sequential accu-

mulation of matrix, fiber damage and delaminations is investigated. Other recent works on inter-laminar stress analysis, multiscale modeling and composite damage characterization are described respectively in Yiming, Sheng and Yejie (2008), in Raimondo and Aliabadi (2009), in Balhi, Vrellos, Drinkwater, Guild, Ogin and Smith (2006) and in Forghani, Zobeiry, Vaziri, Poursartip,and Ellyin (2009). An interesting work considering meshfree modeling and homogenization of 3D orthogonal woven composites has been developed by Wen and Alibadi (2011).

The aim of the present paper, which describes the continuation of the research work on composite grid structures introduced in Tessitore, and Riccio (2005), is to perform a numerical investigation of the failure mechanisms and their interaction in composite grid structures, under compression loading condition, focusing on a Representative Volume Element (RVE). RVE, of course, cannot provide indications about specific complex geometry or boundary conditions of the grids but has the strong advantage to easily represent the basic structural behavior of grids components with onset and propagation of damage in ribs and skin. The compressive structural behavior of the grid RVE has been numerically investigated by means of a geometrically non-linear Finite Element approach (Caputo, Lamanna, and Soprano 2006; Armentani, Calì, Caputo, Cricrì, and Esposito 2006; Caputo, Esposito, Perugini, and Santoro 2002), able to account for fibers and matrix damage onset and propagation, already applied and validated against experimental results for the study of composite joints (Riccio, and Marciano 2005; Riccio 2005), flat delaminated composite panels (Riccio, and Pietropaoli 2008) and stiffened delaminated composite panels (Pietropaoli, and Riccio 2011). This numerical procedure, based on the Hashin's failure criteria to detect the damage on-set and on the ply discount material properties degradation rules to follow the damage progression, has been implemented in the research oriented FEM code B2000 (Merazzi, and de Boer 1994). In order to analyze the damage onset and progression in the skin and in the ribs, two different types of RVE have been considered, with skin and without skin respectively. Numerical analyses performed on these RVE's, with and without considering the damage progression allowed to investigate the failure mechanisms in the skin and in the ribs separately. The obtained results have been compared and assessed in order to evaluate the influence of damage onset and progression on the compression behavior of the analyzed grid structures RVE. The damage status over the RVE has also been assessed to give a realistic representation of the damage initiation and propagation during the loading process. In the next sections, the theory behind the proposed progressive failure approach is described in detail, together with the numerical applications. Then the most relevant results are presented and critically discussed.

2 Theoretical Background

The simulation of the damage on-set and propagation in composite structures needs the simultaneous application of stress based failure criteria and material properties degradation rules. In the next subsection the theory behind the failure criteria and the material properties degradation rules, used in the proposed model, is described in details.

2.1 Failure Criteria

The Hashin's failure criteria have been selected for the present application and implemented in the B2000 FEM code, since, such criteria, using distinct polynomials associated to different failure modes, are able to separately predict the fiber breakage and the matrix cracking for each layer. As a first approximation only the fiber and matrix failure mechanisms have been included in the adopted FEM tool. The instability at fiber level, extensively studied by Berbinau, Soutis, and Guz (1999), has been taken into account through a specific fiber kinking failure criterion while the delamination onset and growth have not been included in the present model, which, as a matter of the facts, has been used to perform a basic, and limited, investigation on intra-laminar composite grid structures failure mechanisms focusing on some of the main aspects characterizing the failure of pristine grid structures under compression. Hence in our analyses, the following failure mechanisms in skin and ribs and the associated failure criteria have been considered (σ_{ij} are the stress components in the ij direction and $S_{ij}, Y_t, X_t, Y_c, X_c$ are the material strengths of the ply):

Matrix tens. fail. ($\sigma_{yy} > 0$)

$$\left(\frac{\sigma_{yy}}{Y_t}\right)^2 + \left(\frac{\sigma_{xy}}{S_{xy}}\right)^2 + \left(\frac{\sigma_{yz}}{S_{yz}}\right)^2 \geq 1 \tag{1}$$

Matrix comp. fail. ($\sigma_{yy} < 0$)

$$\left(\frac{\sigma_{yy}}{Y_c}\right)^2 + \left(\frac{\sigma_{xy}}{S_{xy}}\right)^2 + \left(\frac{\sigma_{xz}}{S_{yz}}\right)^2 \geq 1 \tag{2}$$

Fibre tens. fail. $\sigma_{xx} > 0$

$$\left(\frac{\sigma_{xx}}{X_t}\right)^2 + \left(\frac{\sigma_{xy}}{S_{xy}}\right)^2 + \left(\frac{\sigma_{xz}}{S_{xz}}\right)^2 \geq 1 \tag{3}$$

Fibre comp. fail. $\sigma_{xx} < 0$

$$\left(\frac{\sigma_{xx}}{X_c}\right) \geq 1 \tag{4}$$

Fib-mat sh-out fail. $\sigma_{xx} < 0$

$$\left(\frac{\sigma_{xx}}{X_t}\right)^2 + \left(\frac{\sigma_{xy}}{S_{xy}}\right)^2 + \left(\frac{\sigma_{xz}}{S_{xz}}\right)^2 \geq 1 \tag{5}$$

Fibre-Kinking failure $\sigma_{xx} < 0$

$$\left(\frac{\sigma_{xx}}{X_c}\right)^2 + \left(\frac{\sigma_{xz}}{S_{xz}}\right)^2 \geq 1 \tag{6}$$

In order to find the ply strengths starting from the fibre and matrix properties, micromechanics relations (Stellbrink Kuno 1996) have been adopted.

2.2 Material properties degradation rules

Material properties degradation rules have been applied to take into account the material behaviour of each layer after damage occurrence. This was needed in order to perform a progressive failure analysis up to the global failure, which is assumed to occur when the structure is not able to withstand the load anymore due to the presence of extended degraded areas. For each of the above described failure modes, according to the ply discount approach, an appropriate properties degradation, which roughly reflects the physics of the damage mechanisms, has been introduced.

Matrix tensile and compression failure

$$\begin{aligned} \bar{E}_y &= k \cdot E_y \\ \bar{E}_z &= k \cdot E_z \\ \bar{G}_{yz} &= k \cdot G_{yz} \end{aligned} \tag{7}$$

Fiber tensile and compression failure

$$\begin{aligned} \bar{E}_x &= k \cdot E_x \\ \bar{G}_{xy} &= G_{yz} \\ \bar{G}_{xz} &= G_{yz} \end{aligned} \tag{8}$$

Fiber-matrix shear-out failure

$$\begin{aligned} \bar{G}_{xy} &= G_{yz} \\ \bar{G}_{xz} &= G_{yz} \end{aligned} \tag{9}$$

Fiber-Kinking failure

$$\begin{aligned} \bar{E}_x &= k \cdot E_x \; \bar{G}_{xy} = k \cdot G_{yz} \\ \bar{E}_y &= k \cdot E_y \; \bar{G}_{xz} = k \cdot G_{yz} \\ \bar{E}_z &= k \cdot E_z \; \bar{G}_{yz} = k \cdot G_{yz} \end{aligned} \tag{10}$$

where k is a degradation factor and the over-lined properties indicate the corresponding degraded composite ply material properties. Indeed several formulations can be found in literature which propose different relations for k as a function of the stress state. However, as a first approximation, in this paper the instantaneous unloading approach has been adopted since it has been proved to effectively mimic the brittle material behavior. The instantaneous unloading approach requires that k=0, however a non-zero value for the factor k has been adopted to avoid convergence problems. The composite ply properties have been evaluated starting from the fiber and matrix elastic properties by means of micromechanics relations similarly to what have been done by Riks (1984).

3 Finite Element Implementation

The failure criteria and the properties degradation rules described in the previous section have been implemented in the Finite Element Code B2000 (Merazzi, and de Boer 1994) which is a fully customizable FEM code particularly suitable for research purposes. In particular a progressive damage finite element able to simulate the damage onset and progression has been developed. This finite element is embedded within the B2000 continuation macro-processor which adopts the continuation method of Riks (Gan, Gibson, and Newaz 2004) to perform geometrically non-linear analyses. A flowchart describing the progressive damage procedure, implemented in the FEM code B2000, is shown in Figure 1.

According to the progressive damage procedure, after the application of the initial loading condition, the stiffness matrix, the force vector and stresses are calculated. Then a check of the Hashin failure criteria is performed. If damage is detected, the material properties are degraded according to the properties degradation rules. Convergence is checked and the loop is repeated until the complete failure has been detected. Additional B2000 modules have been developed which are able to handle the huge amount of data coming from the computations (damage location and failure mode for each layer, for each element at each time step).

An integer number has been associated to each failure mode according to Table 1.

This association makes it possible to visualize the damage status, location and failure mechanism as a contour plot over the defined integer range on the un-deformed or deformed structural configurations.

4 Numerical Application

The implemented progressive damage approach has been applied to a Representative Volume Element of a composite grid structure with and without skin. In this section the RVE model is described in detail and the results of the non-linear

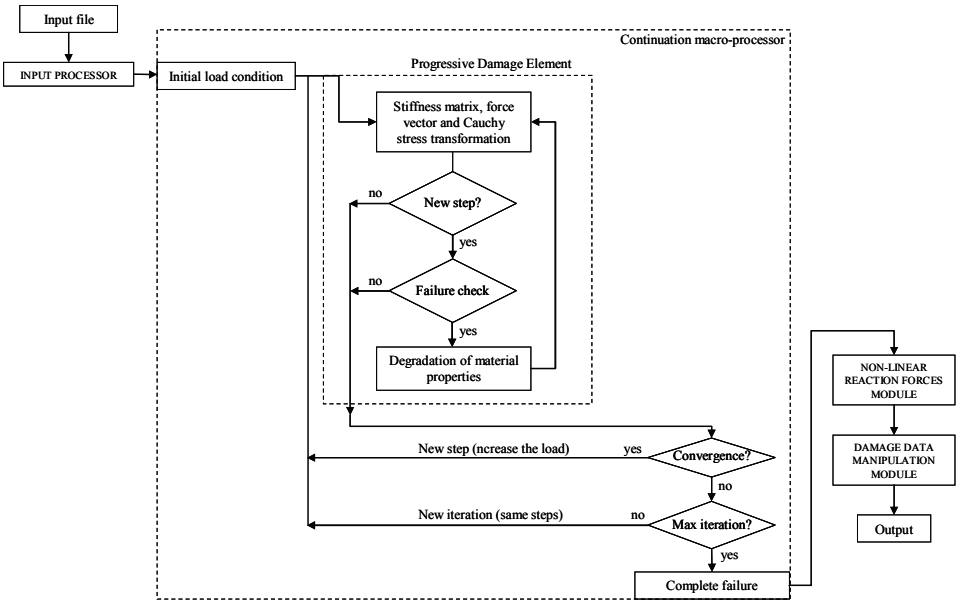

Figure 1: Schematic description of the non linear procedure adopted with damage propagation

Table 1: Numbering of the failure mode in the B2000 code

Failure Mode	**B2000 output**
Undamaged ply	2
Matrix Failure	5
Fibre Failure	6
Shear-out+fibre+matrix failure	7
Kinking Failure	8
Shear-out+matrix failure	9
Matrix+fibre failure	10
Completely failed ply	11

analyses are presented.

4.1 Model geometry, boundary conditions and FEM model

An example of cylindrical composite grid structure obtained by filament winding is shown in Figure 2.

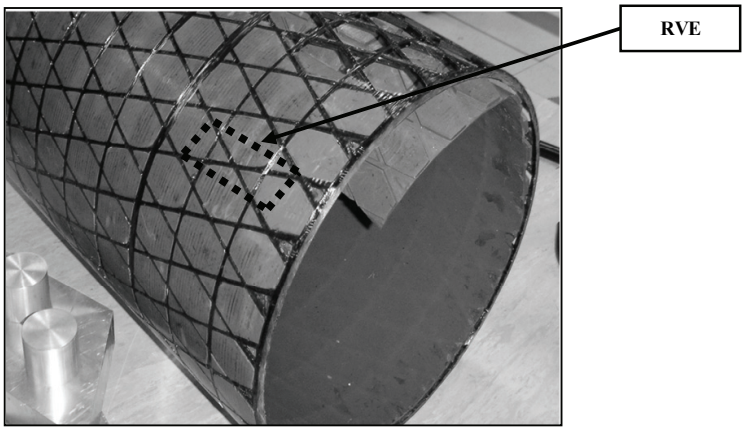

Figure 2: Identification of a Representative Volume Element

The repetitiveness of this structure allows to easily define a Representative Volume Element (RVE). For high Diameter/RVE length ratio (see Figure 3) a simplified plain RVE model can be considered. Also the boundary conditions can be simplified by considering a uniaxial compressive load as representative of the actions undergone by the RVE as a part of the global composite grid structure.

These simplifications can be considered acceptable for the purposes of this study which is aimed to perform a preliminary investigation of the damage onset and propagation in composite grid structures under compression. The geometrical description and the boundary conditions of the plane RVE, subjected to a uniaxial compression load are shown in Figure 3.

The RVE has been completely clamped at y=0. The x=0 and x=b sides are completely free while an imposed displacement has been applied at y=h. Furthermore the displacement along z has been blocked at y=h. The geometrical parameters chosen for the model under consideration are: b = 36.06 mm; θ = 70.17°; so = 4 mm; sd = 4 mm; z1 = 0.5 mm; z2 =4 mm; h1 = 25 mm; h2 = 50 mm.

The stacking sequence in the diagonal ribs and in the intersections between two ribs depends on the chosen winding angle (θ). The winding angle has been set to

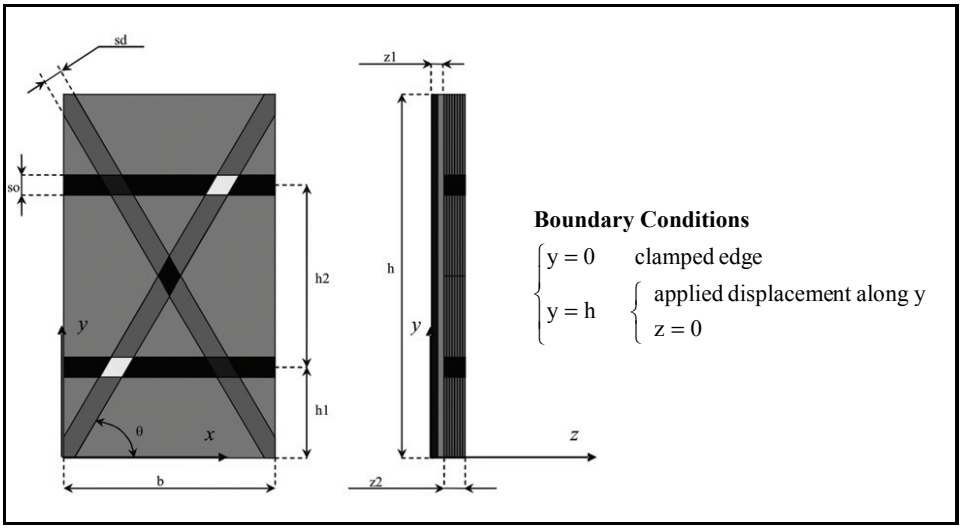

Figure 3: RVE geometry and boundary conditions

Table 2: Ply orientation for each RVE component

Component	Stacking sequence
Skin	[80° / 80° /– 80° /– 80°]
Horizontal ribs	[0,0 / 0,0 / 0,0 / 0,0]
Diagonal ribs	[θ,θ / θ,θ / θ,θ / θ,θ] or [–θ,–θ / –θ,–θ / –θ,–θ / –θ,–θ]
Intersection horizontal/diagonal left-down and right-up	[θ,θ / 0,0 / θ,θ / 0,0]
Intersection horizontal/diagonal right-down and left-up	[-θ,–θ / 0,0 /- θ,–θ / 0,0]
Intersection diagonal/diagonal	[-θ,–θ / θ,θ /–θ,–θ / θ,θ]

be zero for the horizontal ribs and 80˚ for the skin (in general an angle close to 90˚ is chosen for the skin in order to limit skin-rib debonding). A summary of the ply orientation in the different RVE components is given in Table 2.

Starting from the experimentally determined fibre and matrix properties of Table 3, it is possible to derive, the material properties of a single ply (see table 4) by using the micromechanical approach and in particular the modified rule of mixture.

At the ribs' intersection a different volumetric fraction (Vf=0.8) has been considered with respect to the remaining components of the structure (Vf=0.4) in order to achieve a constant thickness along the ribs length.

Table 3: Fiber and Matrix material properties

Fiber and Matrix Elastic Properties		
Fiber Longitudinal Young Modulus	$E_{f,1}$	80 Gpa
Fiber Transverse Young Modulus	$E_{f,2}$	11.7 Gpa
Matrix Young Modulus	E_m	4.3 Gpa
Matrix Ultimate Tension Strain	e^u_m	6%
Fiber Ultimate Fracture Strain	e^u_f	2%
Fiber Poisson Ratio	ν_{f12}	0,32
Matrix Poisson Ratio	ν_m	0,3
Fiber Shear Modulus	G_f	9.65 Gpa
Matrix Shear Modulus	G_m	1,6538 Gpa
Matrix Tension Strength	S_m	67.2 Mpa
Fiber Tension Strength	S_f	5,4 Gpa

The volumetric fraction Vf =0.8 is a "trick" adopted in our numerical model only for the ribs intersections because the local increase in thickness due to the filament winding process has been neglected in order to simplify the geometry. In fact, when grid structures are manufactured, this value of volumetric fraction is not reached and the ribs intersections are built thicker to allow for an higher content of resin in order to avoid high stress concentrations.

The RVE geometry has been meshed by using second order brick elements (20 nodes per element). A preliminary sensitivity analysis on RVE finite element mesh has been performed.

In Figure 4 the resulting RVE FEM model is presented. Each brick element includes only plies with the same orientation. Hence the element material properties can be exactly represented by using an orthotropic material model. By adopting this discretization the interfaces between differently oriented plies correspond to the interfaces between different elements, allowing the inter-laminar stresses to be exactly calculated at the nodes.

4.2 Numerical Results

Non-linear static analyses, with and without damage progression have been performed on the selected RVE models (with and without skin), in order to understand the influence of the failure mechanisms on the compressive mechanical behavior

Table 4: Fiber and Matrix material properties

Lamina Elastic Properties			
		V_f=0.8	V_f=0.4
Longitudinal Young Modulus	E_x	64.86 GPa	34.58 GPa
Transverse Young Modulus	E_y	8.77 GPa	5.75 GPa
Out-of-plane Young Modulus	E_z	8.77 GPa	5.75 GPa
In-plane Shear Modulus	G_{xy}	4.9 Gpa	2.46 GPa
Out-of-plane Shear Modulus	G_{xz}	4.9 Gpa	2.46 GPa
Out-of-plane Shear Modulus	G_{yz}	4.9 Gpa	2.46 GPa
In-plane Poisson Ratio	ν_{xy}	0.328	0.328
Out-of-plane Poisson Ratio	ν_{xz}	0.025	0.025
Out-of-plane Poisson Ratio	ν_{yz}	0.3	0.3
Longitudinal Tensile Strength	X_t	1.23 Gpa	657 Mpa
Transverse Tensile Strength	Y_t	13.10 Mpa	48.12 Mpa
Longitudinal Compressive Strength	X_c	1.23 Gpa	657 Mpa
Transverse Compressive Strength	Y_c	63.18 Mpa	57.32 Mpa
In-plane Shear Strength	$S_{xy=}S_{xz}$	53.76 MPa	53.76 MPa
Out-of-plane Shear Strength	S_{yz}	347 Mpa	153 Mpa

of skin and ribs in composite grid structures. In this subsection these analyses are described in detail and the results are compared and discussed.

4.2.1 Analysis without damage propagation on the Skinned RVE

The mechanical behavior of the skinned grid structure, shown in Figure 3, loaded in compression by applying a displacement of 1mm in the y-direction has been numerically simulated by performing a geometrically non-linear static analysis.

Figure 5 presents the deformed shapes with the out-of-plane displacements contour plots obtained by the non-linear static analysis at different load steps. Figure 5(a) shows the local buckling of the skin in the side bays occurring for an applied load of about 1427 N, while in Figure 5(b) the local buckling of the skin in the upper and lower bays occurring at 6697 N is shown.

Figure 5(c) and Figure 5(d) respectively present the deformed shape at the global

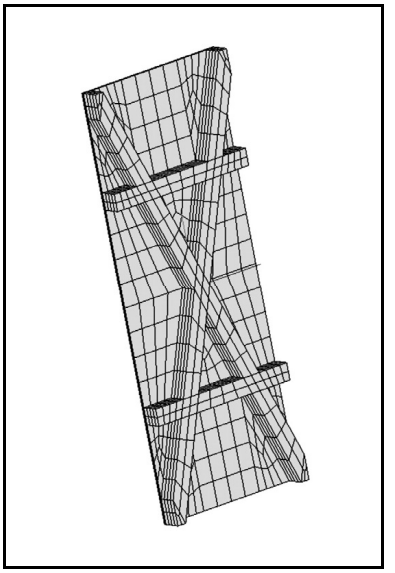

Figure 4: RVE FEM model

buckling of the RVE (occurring at 8167 N) and the post buckling deformed shape (applied load of 8660 N).

In Figure 6(a) the load-displacement curve is presented. This figure does not clearly show the buckling onset of the structure; hence, the axial stiffness as function of the load has been plotted in Figure 6(b). At 1427 N, a first drop down in the axial stiffness of the structure can be pointed out. Such decrease is representative of the local buckling of the skin side bays. A second drop down in the axial stiffness, occurring at about 8167 N, can be associated to the buckling of the ribs (global buckling). From the analysis of figures 6(a) and 6(b) the buckling load of the skin (local buckling) starts for an applied displacement of about 0.07mm while the buckling load of the ribs (global buckling) initiates for an applied displacement of 0.57mm. In Figure 6(c) the out-of-plane displacement curve as function of the applied load is shown. The out-of-plane displacements have been evaluated at (x,y) = (0, h/2) and (x,y) = (b, h/2). Since a perfect overlap in the out-of-plane displacements at the monitored positions has been found, only one curve has been reported in the Figure 6(c). the buckling on-set of the skin side bay (local buckling) and the buckling on-set in the ribs (global buckling) can be easily appreciated.

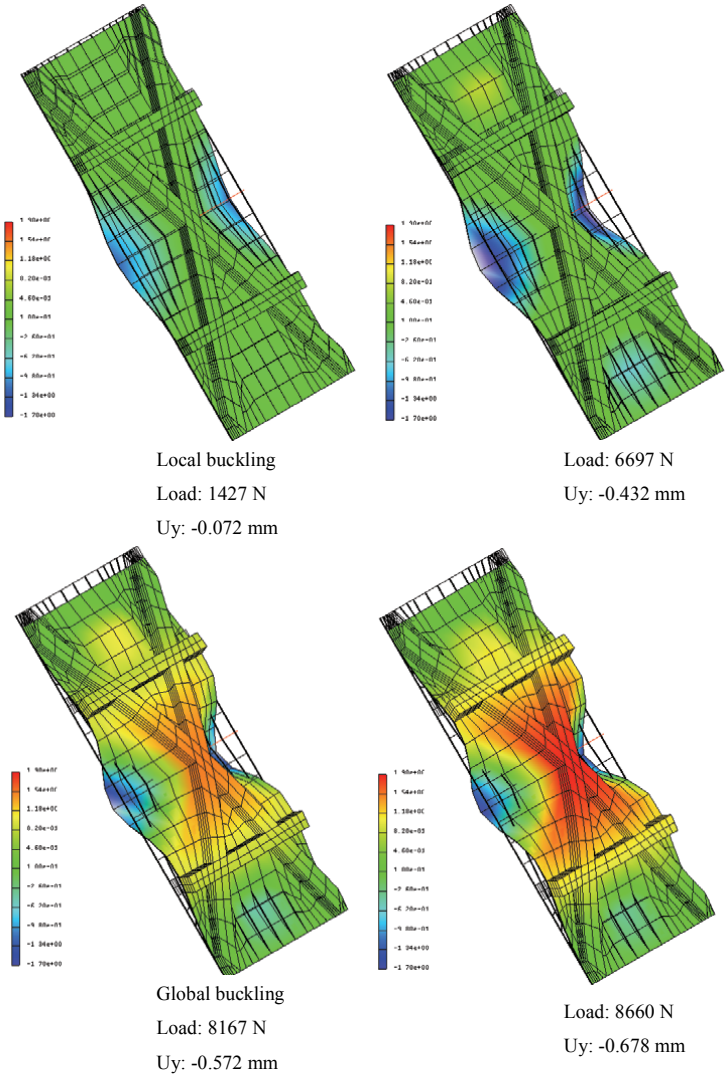

Figure 5: Analysis without damage propagation on the skinned RVE – deformed shapes at different load steps

4.2.2 Analysis with damage propagation on the Skinned RVE

The compression behavior of the skinned RVE shown in the previous subsection is not realistic since the damage in matrix and fibers, expected to occur as a conse-

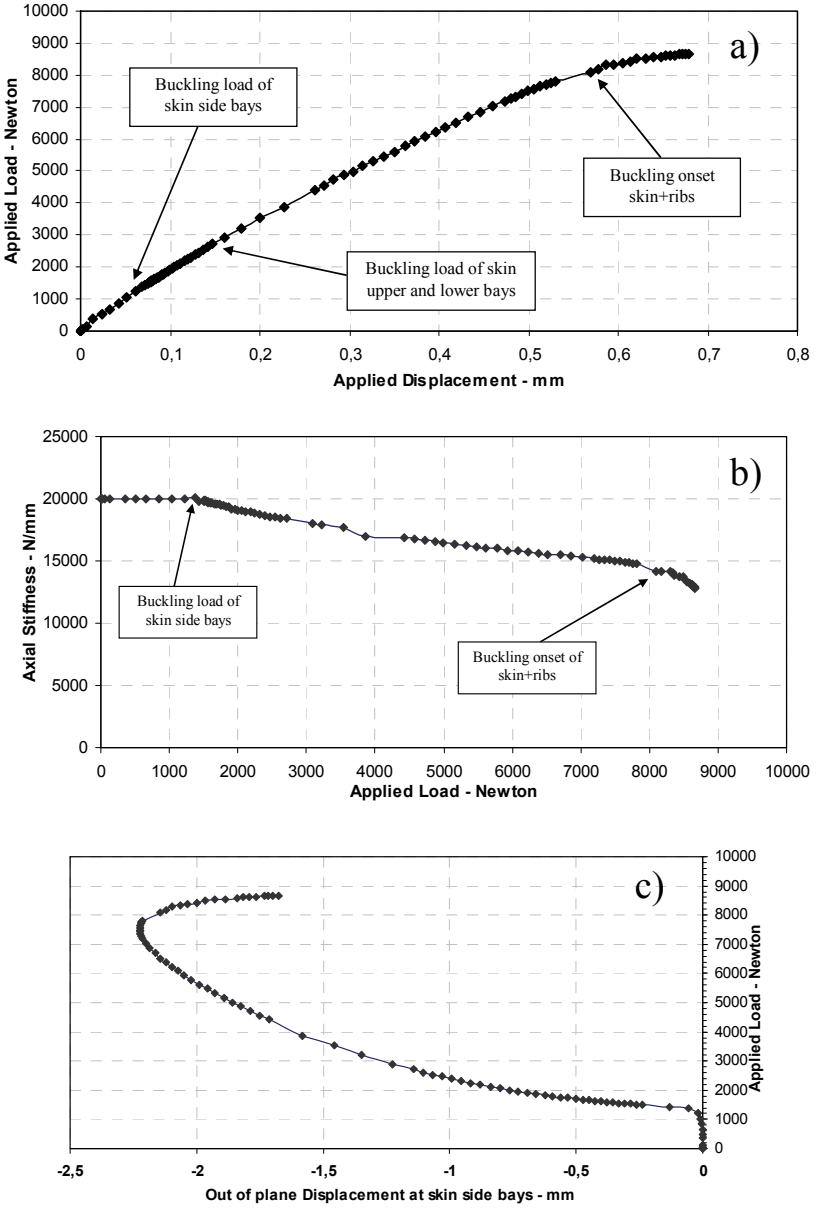

Figure 6: Analysis without damage propagation on the skinned RVE; a) - load/applied displacement curve; b) load/axial stiffness curve; c) load/out-of-plane displ. curve

quence of the skin buckling, has not been taken into account. In order to investigate the mechanical behavior of grid structures when damage onset and propagation occur, a geometrically non-linear analysis with an applied displacement of 1mm in the y-direction has been performed by adopting the implemented progressive damage approach described in section 3.

The results of the non-linear static analysis with damage propagation in terms of fibers and matrix breakage are shown in figures 7 and 8.

In Figure 7 the deformed shapes of the non-linear static analysis with damage propagation at different load steps are reported for both 80° and –80° oriented plies. In order to show the B2000 outputs in terms of damage growth, the integer values of Table 1 have been used to represent the failure mode in the ply.

According to Figure 7 no damage has been detected up to the local buckling. The damage on-set, consisting of both matrix and fiber breakage, has been found for an applied load of 4263 N. The damage propagates as fiber and shear out failure that affects only the skin but has an impact on the whole structure load carrying capability. Indeed, by increasing the displacement in the y-direction, the skin suddenly reaches the collapse for an applied displacement of 2,757mm (load of 4169 N).

In practice, the collapse load obtained by this procedure takes into account the damage onset and propagation in the skin and shows that the skin is of main concern for the integrity of the whole grid structure. This global failure is reached approximately at the 50% of the global buckling load found without considering the failure. This is a proof of the relevance of the failure onset and propagation when simulating the mechanical behavior of composite grid structures. Figure 8(a) (load-displacement curve) and Figure 8(b) (axial stiffness as a function of the load) show that the local buckling of the skin, as for the analysis with damage propagation, occurs at about 1427 N. The damage onset is not visible in this figures while a sudden drop in the load carrying capability and in the axial stiffness show the final failure of the RVE.

In Figure 8(c) the out-of-plane displacement curves as function of the applied load is reported. The out-of-plane displacement is evaluated at (x,y) = (0, h/2) and (x,y) = (b, h/2).

No appreciable difference can be observed with respect to the no-damage approach in terms of out of plane displacements and local buckling value.

4.2.3 Analysis with damage propagation on the RVE without skin

Sometimes, the grid structures are manufactured with very thin skins which, differently from the previously analyzed configurations, does not contribute significantly to the global load carrying capability, hence the global failure is driven by

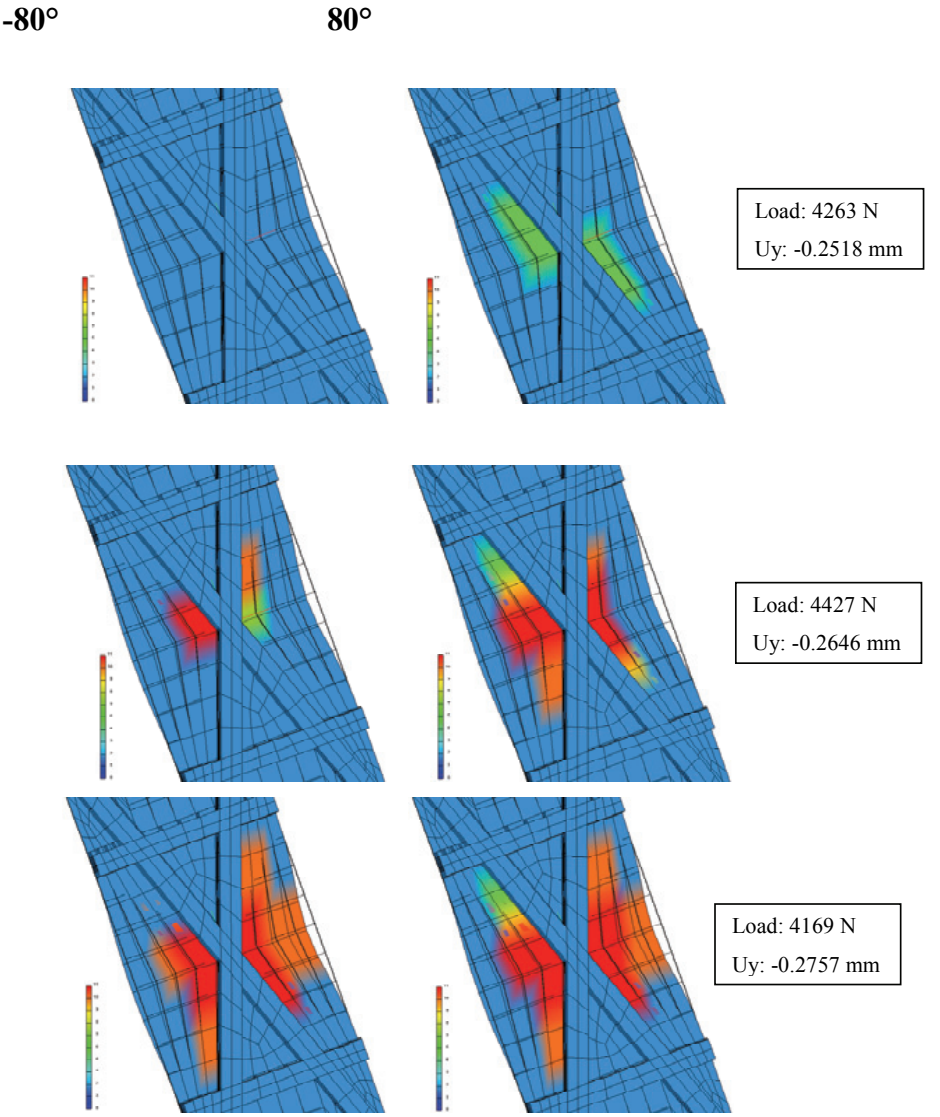

Figure 7: Analysis with damage propagation on the skinned RVE – deformed shapes with failure modes contours at different load steps

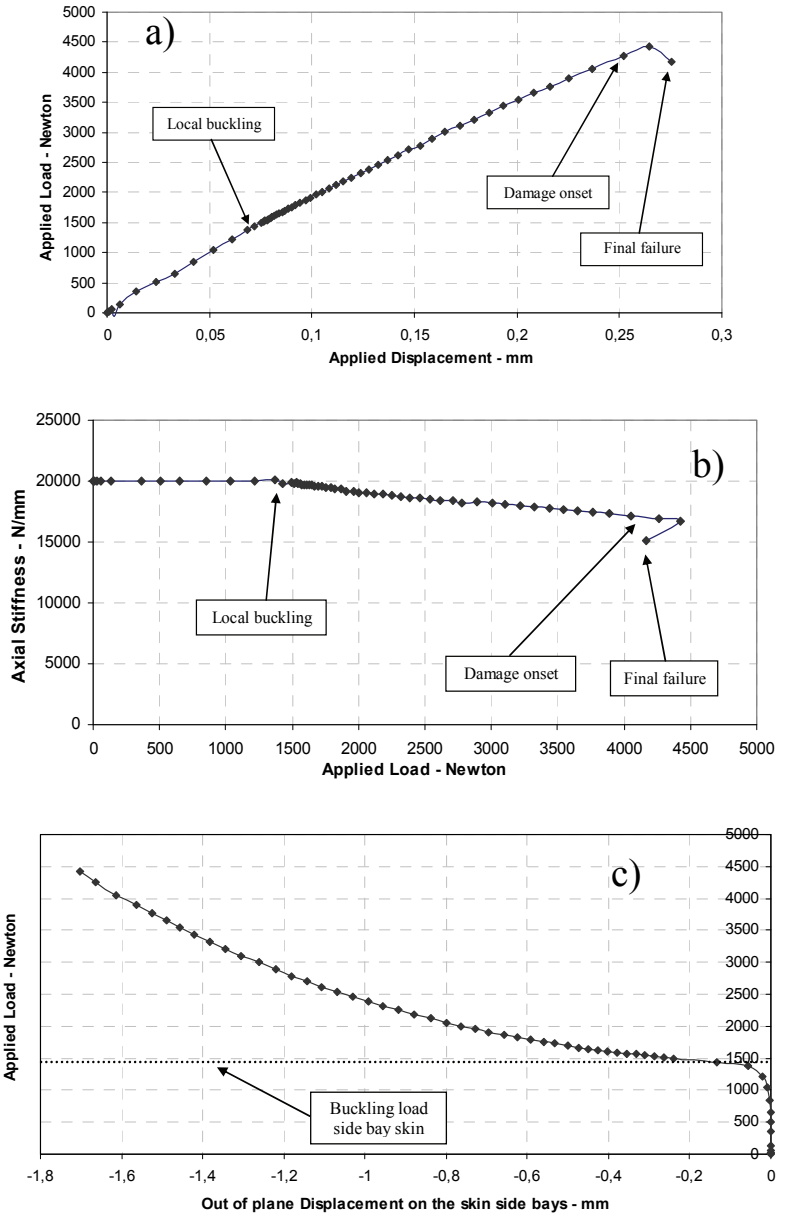

Figure 8: Analysis with damage propagation on the skinned RVE: a) - load/applied displacement curve; b) load/axial stiffness curve; c)load/out-of-plane displacement curve

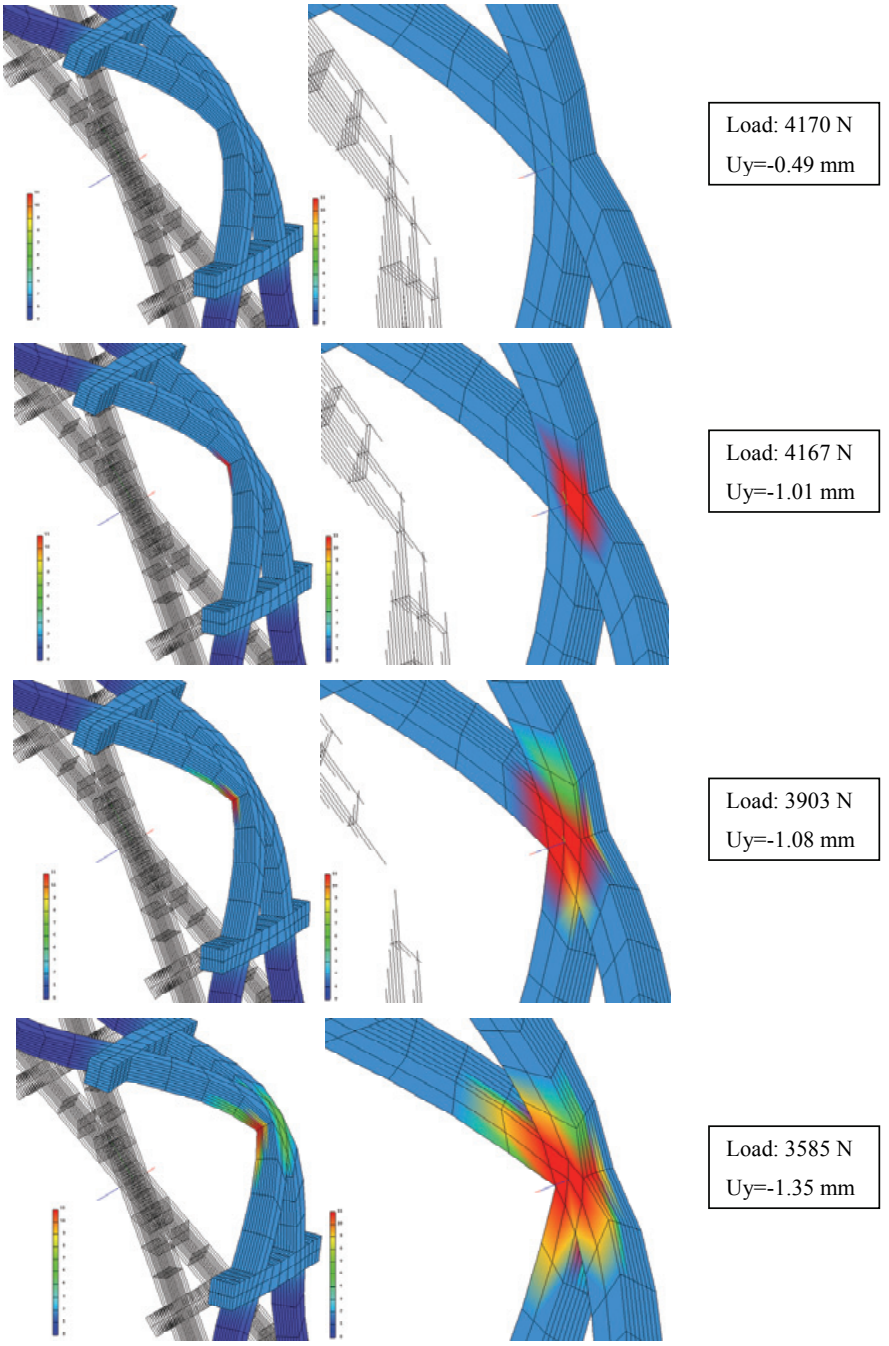

Figure 9: Analysis with damage propagation on the RVE without skin – deformed shapes with failure modes contours at different load steps

the damage in the ribs. In this subsection, in order to investigate the damage onset and evolution in the ribs of composite grid structures, an application of the proposed progressive damage approach to an RVE without skin is presented. The RVE shown in Figure 3 without the skin has been loaded in compression by applying a displacement of 3mm in the y direction. A geometrically non-linear analysis has been performed by taking into account the damage onset and progression in terms of fiber breakage and matrix cracking. In figure 9 the deformed shapes at different time steps are presented. The damage propagation contours (plotted according to the values of Table 1) provide a description of the damage evolution during the loading process. Fiber, matrix and shear-out failure initiates in the back of the intersection between two diagonal ribs after the buckling occurring at 4170 N. Quickly the damage propagates along the thickness and fiber failure becomes visible. When complete failure of the structure is detected, the load carrying capability is reduced (load at failure of 3585 N) and about the 80% of the plies in the intersection between the diagonal ribs are completely broken.

In figure 10(a) the load-displacement curve is shown. The buckling onset at 4170 N is visible together with the decrease in load carrying capability before failure. In figure 10(b) the axial stiffness as a function of the load is presented. Once again the reduction in stiffness associated with the buckling phenomenon can be appreciated. Finally, figure 10(c) shows the load-out-of-plane displacement curve at the intersection between the two diagonal ribs. The global buckling and the loss of load carrying capability is clearly pointed out.

5 Conclusions

In this paper the damage on-set and propagation in terms of fiber and matrix breakage on a composite grid structure Representative Volume Element have been investigated. A progressive damage model implemented in the Finite Element code B2000 has been used for computations. Geometrically non-linear structural analyses both in presence of damage and not have been carried out on the composite RVE with skin and without skin, in order to understand the influence of damage onset and propagation respectively in skin and ribs on the compression behavior of composite grid structures. The results for the skinned RVE show that no appreciable differences have been found between the damage and the no-damage approach up to the local buckling of the skin, while the fiber and matrix breakage considerably affect the post buckling behavior. The damage on-set in terms of matrix cracking takes place very soon during the loading process and the propagation of damage in terms of shear-out and ply complete failure lead to a premature collapse of the skin and consequently of the complete skinned RVE. The results obtained for the grid without skin (lattice structure) show matrix cracking on-set occurring

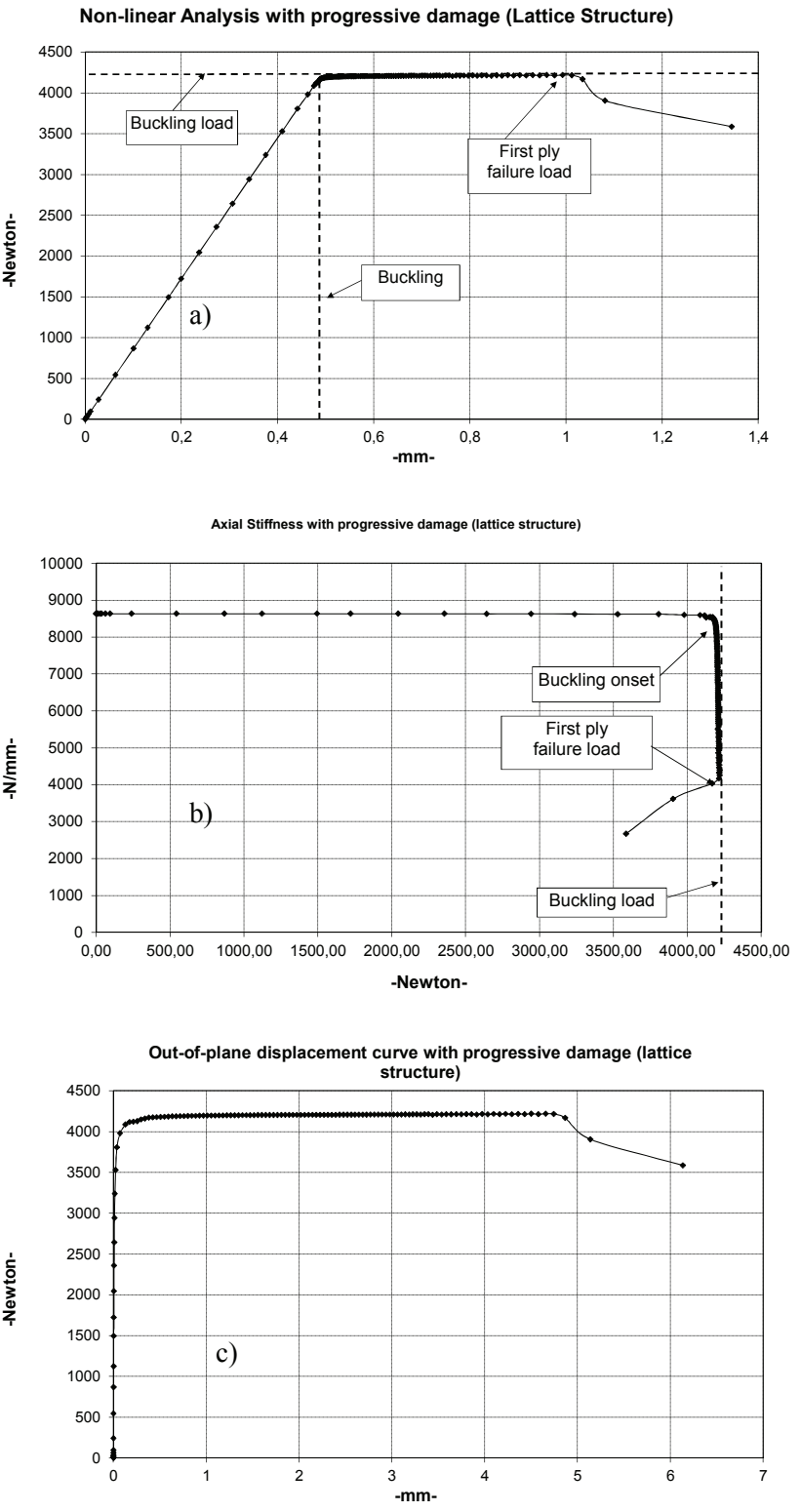

Figure 10: Analysis with damage propagation on RVE without skin: a) load/applied displacement curve; b) load/axial stiffness curve; c)load/out-of-plane displacement curve

after the rib buckling load between the diagonal ribs. Then fiber breaking and ply complete failure propagate all along the thickness causing the diagonal ribs failure. Indeed, the information on damage evolution in composite grid structure obtained by applying the proposed progressive damage model, already applied and validated against experimental results, to a simplified RVE subjected to simplified loading and boundary conditions could provide a first insight on the failure mechanisms occurring when dealing with this kind of structures. These first information will be useful to start a more focused numerical and experimental test campaign finalized to the investigation of failure mechanisms in composite grid structures. However the inclusion of more complex boundary conditions and of delaminations onset and propagation in the proposed damage model, represents an interesting subject for future developments, aimed to a more detailed understanding of composite grid structures failure mechanisms.

References

Armentani, E., Calì, C., Caputo, F., Cricrì, G., Esposito, R. (2006): Numerical solution techniques for structural instability problems. *Journal of Achievements in Materials and Manufacturing Engineering*, vol. 19-1, pp. 53-64.

Balhi, N., Vrellos, N.; Drinkwater, B.W.; Guild, F.J.; Ogin, S.L.; Smith, P.A. (2006) Intra-laminar cracking in CFRP laminates: observations and modelling *Source: Journal of Materials Science*,v 41, n 20, p 6599-609.

Berbinau, P., Soutis, C., Guz, I. A. (1999): Compressive failure of 0° unidirectional CFRP laminates by fibre microbuckling. *Composites Sci. & Technol.*, vol. 59(9), pp. 1451-1455.

Buragohain, M., Velmurugan, R. (2011): Study of filament wound grid-stiffened composite cylindrical structures. *Compos Struct*, vol. 93, pp. 1031-1038.

Caputo, F., Esposito, R., Perugini, P., Santoro, D. (2002): Numerical-experimental investigation on post-buckled stiffened composite panels. *Composite Structures*, vol. 55/3 pp. 347-357.

Caputo, F., Lamanna, G., Soprano, A. (2006): Numerical Investigation on the Crack Propagation in a Flat Stiffened Panel. *Key Engineering Materials*, vol. 324-325, pp. 559-562.

Christensen, R.M. (1988): Tensor Transformation and Failure Criteria for the Analysis of Fibre Composite Materials. *J. of Comp. Mat.*, vol. 22, pp. 874-897.

Feng, W.W. (1991): A Failure Criterion for Composite Materials. *J. of Comp. Mat.*, vol. 25, pp. 88-100.

Forghani, A., Zobeiry, N.; Vaziri, R.; Poursartip, A.; Ellyin, F. (2009): A con-

sistent framework for formulation and characterization of a sub-laminate based damage model. *17th International Conference on Composite Materials.ICCM-17.*

Fu, Yimin, Li, Sheng; Jiang, Yejie (2008): Analysis of inter-laminar stresses for composite laminated plate with interfacial damage. *Acta Mechanica Solida Sinica,* v 21, n 2, p 127-140.

Gan, C., Gibson, RF., Newaz, G.M. (2004): Analytical/Experimental Investigation on Energy Absorption in Grid-stiffened Composite Structures under Transverse Loading. *Experimental Mechanics*, vol. 44/2, pp. 185-194.

Hahn, H.T., Tsai, S.W. (1983): On the Behaviour of Composite Laminates After Initial Failures. Astronautics and Aeronautics, vol. 21, pp. 58-62.

Hashin, Z. (1980): Failure Criteria for Unidirectional Fiber Composites. ASME Journal of Applied Mechanics, vol. 47, pp. 329-334.

Hashin, Z., Rotem, A. (1973): A Fatigue Failure Criterion for Fibre Reinforced Materials. *Journal of Composite Materials*, vol. 7, pp. 448-474.

He, J.-X., He, G.-Q. (2010): Strength analysis of composite grid stiffened structure. *Guti Huojian Jishu/Journal of Solid Rocket Technology*, vol. 33/4, pp. 449-458.

Hou, A., Gramoll, K. (2000): Fabrication and compressive strength of the composite attachment fitting for launch vehicle. J Adv Mater, vol. 32/1, pp. 39-45.

Huybrechts, S.M., Meink, T.E., Wegner, P.M., Ganley, J.M. (2002): Manufacturing theory for advanced grid stiffened structures. *Comp Part A: Applied Science and Manufacturing*, vol. 33/2, pp. 155-161.

Kashtalyan, M., Soutis, C. (2005): Analysis of composite laminates with intra- and interlaminar damage. *Progress in Aerospace Science*, vol. 41, pp. 152-173.

Katerelos, D.T.G., Kashtalyan, M., Soutis, C., Galiotis, C. (2008): Matrix cracking in polymeric composites laminates: Modelling and experiments. *Composites Science and Technology*, vol. 68, pp. 2310-2317.

Kidane, S., Helms, GLiJ., Pang, S., Woldesenbet, E. (2003): Buckling load analysis of grid stiffened composite cylinders. *Comp: Part B*, vol. 34, pp. 1-9.

Li, L.Y. , Wen, P.H.; Aliabadi, M.H (2011): Meshfree modeling and homogenization of 3D orthogonal woven composites. *Composites Science and Technology*, v 71, n 15, p 1777-1788, 24.

Merazzi, S., de Boer, A. (1994): B2000 Manuals. SMR Corp.

Murray, Y., Schwer, L. (1990): Implementation and Verification of Fiber Composite Damage Models, Failure Criteria and Analysis in Dynamic Response. ASME AMD, vol. 107, pp. 21-30.

Nahas, M.N. (1986): Survey of Failure and Post-Failure Theories of Laminated Fibre Reinforced Composites. *Journal of Composites Technology and Research*, vol. 8, pp. 138-153.

Ochoa, O.O., Reddy. J.N. (1992): Finite Element Analysis of Composite Laminates. Kluwer Academic Publishers, Dordrecht, The Netherlands.

Petit, P.H., Waddoups, M.E. (1969): A Method of Predicting the Non-Linear Behaviour of Laminated Composites. *J. of Comp. Mat.*, vol. 3, pp. 2-19.

Pietropaoli, E., Riccio, A. (2011): A Global/Local Finite Element Approach for Predicting Interlaminar and Intralaminar Damage Evolution in Composite Stiffened Panels Under Compressive Load. *Applied Composite Materials*, vol. 18/2, pp. 113-125.

Raimondo, L., Aliabadi, M.H. (2009): Multiscale progressive failure analysis of plain-woven composite materials, *Journal of Multiscale Modeling*, v 1, n 2, p 263-301.

Riccio, A., Marciano, L. (2005) Effects of Geometrical and Material Features on Damage Onset and Propagation in Single-lap Bolted Composite Joints under Tensile Load: Part I – Experimental Studies. *Int. Journal of Composite Materials*, vol. 39/23, pp. 2071-2090.

Riccio, A. (2005): Effects of Geometrical and Material Features on Damage Onset and Propagation in Single-lap Bolted Composite Joints under Tensile Load: Part II – Numerical Studies. *Int. Journal of Composite Materials*, vol. 39/23, pp. 2091-2112.

Riccio, A., Pietropaoli, E. (2008): Modelling damage propagation in composite plates with embedded delamination under compressive load. *Int. Journal of Composite Materials*, vol. 42/13, pp. 1309-1335.

Riks, E. (1984): Progress in collapse analysis. ASME Pressure Vessel and Piping Conference (session on Collapse Analysis of Structures – I), San Antonio, Texas.

Sandhu, R.S. (1974): Non-Linear Behaviour of Unidirectional and Angle Ply Laminates. AIAA Journal of Aircraft, vol. 13, pp. 104-111.

Sleight, D.W., Knight. N.F., Wang, J.T. (1997): Evaluation of a Progressive Failure Analysis Methodology for Laminated Composite Structures. AIAA Paper, 97-1187, AIAA/ASME/ASCE/AHS/ASC Structures, Structural Dynamics, and Materials Conference and Exhibit.

Sleight, D.W. (1999): Progressive Failure Analysis Methodology for Laminated Composite Structures. NASA/TP-1999-209107.

Soutis, C., Kashtalyan, M. (2011): Residual Stiffness of Cracked Cross-Ply Composite Laminates Under Multi-Axial In-plane Loading. *Applied Composite Mate-*

rials, vol. 18, pp. 31-43.

Stellbrink Kuno, K.U. (1996): Micromechanics of Composites. Carl Hanser Verlag, New York.

Tessitore, N., Riccio, A. (2005) Development and application of a progressive damage approach to a grid structure representative volume element. Proceedings of the 10th International Conference on Civil, Structural and Environmental Engineering Computing, Civil-Comp.

Tsai, S.W., Wu, E.M. (1971): A General Theory of Strength for Anisotropic Material. *J. of Comp. Mat.*, vol. 5, pp. 58-80.

Vasiliev, V.V., Barynin, V.A., Rasin, A.F. (2001): Introduction to the design and behavior of bolted joints. *Compos Struct*, vol. 54, pp. 361-370.

Vasiliev, V.V., Razin, A.F. (2006): Anisogrid composite lattice structures for spacecraft and aircraft applications. *Compos Struct*, vol. 76, pp. 182-189.

Wodesenbet, E., Kidane, S., Pang, S. (2003): Optimization for buckling loads of grid stiffened composite panels. *Compos Struct*, vol. 60, pp. 159-169.

Yamada, S.E., Sun, C.T. (1978): Analysis of Laminate Strength and its Distribution. *J. of Comp. Mat.*, vol. 12, pp. 275-284.

Zhang, Z., Chen, H., Ye, L. (2008): Progressive failure analysis for advanced grid stiffened composite plates/shells. *Comp Struct*, vol. 86, pp. 45-54.